

# Negative Ion Photoelectron Spectroscopy Confirms the Prediction that $(\text{CO})_5$ and $(\text{CO})_6$ Each Has a Singlet Ground State

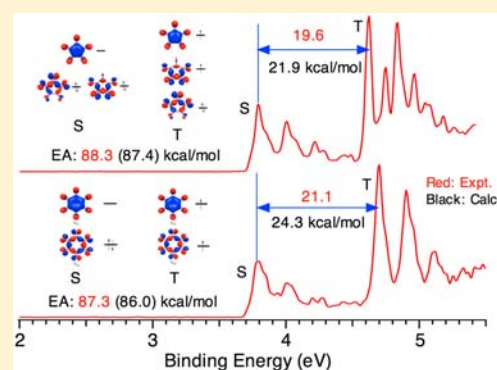
Xiaoguang Bao,<sup>†</sup> David A. Hrovat,<sup>†</sup> Weston Thatcher Borden,<sup>\*,†</sup> and Xue-Bin Wang<sup>\*,‡</sup>

<sup>†</sup>Department of Chemistry and the Center for Advanced, Scientific Computing and Modeling, University of North Texas, 1155 Union Circle, #305070, Denton, Texas 76203-5070, United States

<sup>‡</sup>Chemical & Materials Sciences Division, Pacific Northwest National Laboratory, P.O. Box 999, MS K8-88, Richland, Washington 99352, United States

## Supporting Information

**ABSTRACT:** Cyclobutane-1,2,3,4-tetraone has been both predicted and found to have a triplet ground state, in which a  $b_{2g}$   $\sigma$  molecular orbital (MO) and an  $a_{2u}$   $\pi$  MO are each singly occupied. In contrast,  $(\text{CO})_5$  and  $(\text{CO})_6$  have each been predicted to have a singlet ground state. These predictions have been tested by generating the  $(\text{CO})_5^{\bullet-}$  and  $(\text{CO})_6^{\bullet-}$  radical anions in the gas phase, using electrospray vaporization of solutions of, respectively, the croconate  $(\text{CO})_5^{2-}$  and rhodizonate  $(\text{CO})_6^{2-}$  dianions. The negative ion photoelectron (NIPE) spectrum of the  $(\text{CO})_5^{\bullet-}$  radical anion gives an electron affinity of EA = 3.830 eV for formation of the singlet ground state of  $(\text{CO})_5$ . The triplet is found to be higher in energy by 0.850 eV (19.6 kcal/mol). The NIPE spectrum of the  $(\text{CO})_6^{\bullet-}$  radical anion gives EA = 3.785 eV for forming the singlet ground state of  $(\text{CO})_6$ , with the triplet state higher in energy by 0.915 eV (21.1 kcal/mol). (RO)CCSD(T)/aug-cc-pVTZ// (U)B3LYP/6-311+G(2df) calculations give EA values that are only approximately 1 kcal/mol lower than those measured and  $\Delta E_{ST}$  values that are 2–3 kcal/mol higher than those obtained from the NIPE spectra. Calculations of the Franck–Condon factors for transitions from the ground state of each radical anion,  $(\text{CO})_n^{\bullet-}$  to the lowest singlet and triplet states of the  $n = 4–6$  neutrals, nicely reproduce all of the observed vibrational features in the low-binding energy regions of all three NIPE spectra. Thus, the calculations of both the energies and vibrational structures of the two lowest energy bands in each of the NIPE spectra support the interpretation of the spectra in terms of a singlet ground state for  $(\text{CO})_5$  and  $(\text{CO})_6$  but a triplet ground state for  $(\text{CO})_4$ .



## INTRODUCTION

Although cyclobutane-1,2,3,4-tetraone,  $(\text{CO})_4$ , might be expected to have a closed-shell, singlet ground state, electronic structure calculations have found the lowest triplet state to be either the ground state or very close to it in energy.<sup>1</sup> In the triplet state, one unpaired electron occupies the  $b_{2g}$   $\sigma$  molecular orbital (MO) and another electron, of parallel spin, occupies the  $a_{2u}$   $\pi$  MO. These MOs are shown in Figure 1.

Coupled-cluster calculations predict the triplet to lie below the lowest singlet state of  $(\text{CO})_4$  by 1–2 kcal/mol.<sup>1b–e</sup> It has also been argued that the triplet *must* be the ground state, because the  $b_{2g}$   $\sigma$  MO and the  $a_{2u}$   $\pi$  MO are calculated to have nearly the same energies.<sup>2</sup> Since these MOs are nondisjoint,<sup>3</sup>

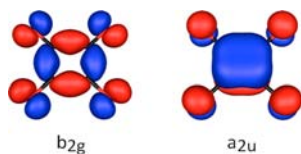


**Figure 1.** Two MOs that are singly occupied in the triplet ground state of  $(\text{CO})_4$ .

Hund's rule<sup>4</sup> should be applicable, thus leading to the unequivocal prediction that  $(\text{CO})_4$  should have a triplet ground state.<sup>2</sup>

This prediction has been recently confirmed by the negative ion photoelectron (NIPE) spectrum of  $(\text{CO})_4^{\bullet-}$ .<sup>5</sup> The energy difference between the triplet ground state and the lowest singlet state was found to be 1.5 kcal/mol, in good agreement with the results of the coupled-cluster calculations.<sup>1b–e</sup>

An obvious question is whether other  $(\text{CO})_n$  molecules have triplet ground states. This question has been recently addressed by a combination of analysis of the MOs of  $(\text{CO})_n$  molecules and B3LYP and CCSD(T) calculations on  $(\text{CO})_n$  with  $n = 2–6$ .<sup>6</sup> It was found that, when  $n$  is an odd number (i.e.,  $n = 2m + 1$ ), the highest occupied MOs are a degenerate pair of  $\sigma$  MOs, with the lowest empty  $\pi$  orbital considerably higher in energy. In agreement with this qualitative analysis of the MOs of  $(\text{CO})_{2m+1}$ ,  $(\text{CO})_3$  and  $(\text{CO})_5$  were in fact each calculated to have a singlet ground state.

**Received:** October 1, 2012

**Revised:** January 16, 2013

**Published:** February 27, 2013

The electronic structures of  $(\text{CO})_n$  molecules with even  $n$  (i.e.,  $n = 2m$ ) were found to be different from those of  $(\text{CO})_n$  molecules with  $n = 2m+1$ . In  $(\text{CO})_2$ ,  $(\text{CO})_4$ , and  $(\text{CO})_6$ , a pair of electrons has to be distributed between two MOs, and the energetic proximity of this pair of MOs determines whether the ground state of  $(\text{CO})_{2m}$  is a singlet or a triplet.

For instance, in  $(\text{CO})_2$ , this pair of MOs is degenerate by symmetry. Therefore, since these MOs are nondisjoint,<sup>3</sup> Hund's rule should apply,<sup>4</sup> and as expected, calculations do indeed predict that  $(\text{CO})_2$  has a triplet ground state.<sup>7</sup>

In  $(\text{CO})_4$ , the  $b_{2g}$  and  $a_{2u}$  MOs shown in Figure 1 are not degenerate by symmetry, but as already mentioned, they are calculated to be very close in energy.<sup>2</sup> The  $\sigma$  bonding between nearest-neighbor carbons in the  $b_{2g}$  MO would be expected to be stronger than the  $\pi$  bonding between nearest-neighbor carbons in the  $a_{2u}$  MO. However, the cross-ring interactions between carbons C1 and C3 and between C2 and C4 are bonding in  $a_{2u}$  but antibonding in  $b_{2g}$ . These two opposing effects, involving nearest-neighbor and cross-ring interactions, almost cancel in  $(\text{CO})_4$ ,<sup>6</sup> and as already noted, the near degeneracy of  $b_{2g}$  and  $a_{2u}$  MOs is what makes the ground state of  $(\text{CO})_4$  both predicted<sup>1b-e,2</sup> and found<sup>5</sup> to be a triplet.

In  $(\text{CO})_6$ , the cross-ring distances between non-nearest neighbor atoms are much larger than those in  $(\text{CO})_4$ , so one would expect the  $b_{2u}$   $\sigma$  MO to be lower in energy than the  $a_{2u}$   $\pi$  MO. This was indeed calculated to be the case, and consequently,  $(\text{CO})_6$ , unlike  $(\text{CO})_4$ , was predicted to have a singlet ground state.<sup>6</sup>

Negative ion photoelectron spectroscopy (NIPES) has been used to test the results of calculations of singlet–triplet energy differences in a wide variety of molecules,<sup>8</sup> including  $(\text{CO})_4$ .<sup>5</sup> In order to test the predictions that  $(\text{CO})_5$  and  $(\text{CO})_6$  both have singlet ground states, the Pacific Northwest National Laboratory (PNNL) researchers have generated  $(\text{CO})_5^{\bullet-}$  and  $(\text{CO})_6^{\bullet-}$  radical anions in the gas phase and obtained their NIPES spectra. In this paper, we present the spectra that were obtained and our analyses of them.

We also present the results of additional CCSD(T) calculations of the energies of the bands in each spectrum and simulations of the vibrational structure in each band (including the bands in the previously published NIPES spectrum of  $(\text{CO})_4^{\bullet-}$ ),<sup>5</sup> based on the results of B3LYP calculations of the Franck–Condon factors (FCFs) for each band. Both types of calculations were carried out by the chemists at the University of North Texas (UNT), in order to confirm the spectral assignments and also to test the ability of the CCSD(T) calculations to duplicate the electron affinities (EAs) and singlet–triplet energy differences ( $\Delta E_{\text{ST}}$ ) that were obtained from the NIPES spectra.

## EXPERIMENTAL AND THEORETICAL METHODS

**Low-Temperature NIPES.** The spectra were obtained, using low-temperature photoelectron spectroscopy, coupled with an electrospray ionization source and a temperature-controlled ion trap, recently developed at PNNL.<sup>9</sup> Spraying approximately 1 mM acetonitrile aqueous solutions of croconate  $(\text{CO})_5^{2-}$  and rhodizonate  $(\text{CO})_6^{2-}$  sodium salts readily generated the respective singly charged radical anions of  $(\text{CO})_5^{\bullet-}$  and  $(\text{CO})_6^{\bullet-}$ , although the majority of anions from the solutions were  $\text{C}_5\text{O}_5\text{H}^-$  and  $\text{C}_6\text{O}_6\text{H}^-$ . The anions were directed by rf devices into a cold ion trap, where they were accumulated and cooled down to 20 K, in order to eliminate vibrational hot bands and achieve optimal spectral resolution.  $(\text{CO})_5^{\bullet-}$  and  $(\text{CO})_6^{\bullet-}$  were carefully mass-selected and then decelerated (to minimize Doppler broadening) before being photodetached with 266 nm (4.661 eV) or

193 nm (6.424 eV) photons. With the lower energy photons, the vibrational structure in the ground state of  $(\text{CO})_5$  and  $(\text{CO})_6$  is better resolved, but with the higher energy photons, excited states can also be accessed, so that singlet–triplet energy differences can be measured. The photoelectron spectra were calibrated using the known spectra of  $\Gamma^-$ ,  $\text{ClO}_2^-$ , and  $\text{Cu}(\text{CN})_2^-$ .

**Computational Methodology.** Geometries of the radical anions and singlet and triplet states of the neutrals were optimized with unrestricted (U)B3LYP calculations,<sup>10</sup> using the 6-311+G(2df) basis set.<sup>13</sup> Frequencies and corrections for zero-point vibrational energy differences were obtained from (U)B3LYP/6-311+G(2df) vibrational analyses. These calculations were performed with the Gaussian09 suite of programs.<sup>14</sup>

Single-point energies were calculated at many different levels of theory. We consider our most reliable results to have been furnished by our largest calculations: (RO)CCSD(T),<sup>15</sup> based on Hartree–Fock (HF) and restricted open-shell (RO)HF reference wave functions, and utilizing the aug-cc-pVTZ basis set.<sup>16</sup> These calculations were performed with the MOLPRO suite of programs.<sup>17</sup>

Simulations of the vibrational structures in the NIPES spectra, based on FCFs, were performed using the ezSpectrum (version 3.0) program developed by Mozhayskiy and Krylov.<sup>18</sup> The necessary equilibrium geometries, harmonic vibrational frequencies, and normal mode vectors for  $(\text{CO})_n^{\bullet-}$  and  $(\text{CO})_n$  ( $n = 4-6$ ) were obtained from (U)B3LYP/6-311+G(2df) calculations.

## RESULTS AND DISCUSSION

**NIPES Spectra of  $(\text{CO})_5^{\bullet-}$  and  $(\text{CO})_6^{\bullet-}$ .** NIPES spectral features represent transitions from the ground states of anions to the ground and excited states of neutrals, along with the associated excited vibrational progressions. The NIPES spectra of the  $(\text{CO})_5^{\bullet-}$  radical anion were obtained at both 266 and 193 nm and are shown in Figure 2a and 2b, respectively.

Two sets of spectral features at electron binding energies (EBEs) between 3.7 and 4.6 eV (X) and between 4.6 and 5.5 eV (A) are observed in Figure 2b, followed by a featureless rising tail at an EBE of greater than 5.5 eV. The origin of each feature has the strongest intensity, and the intensity of band X

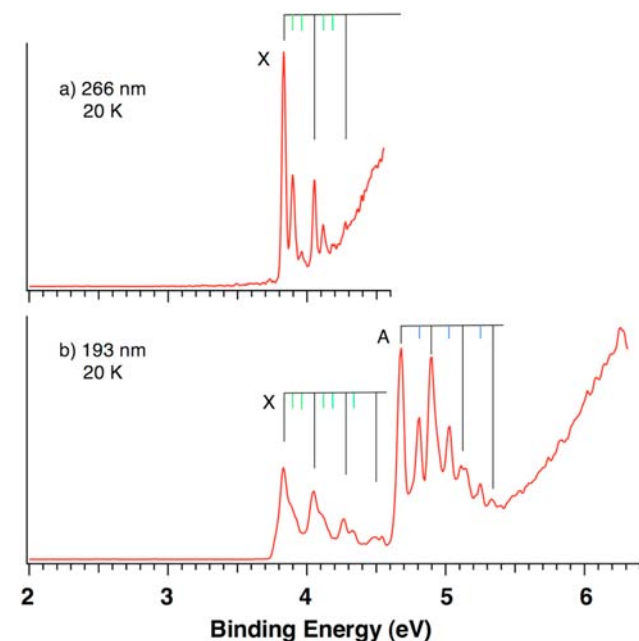


**Figure 2.** Low-temperature (20 K) NIPES spectra of  $(\text{CO})_5^{\bullet-}$  at (a) 266 and (b) 193 nm. The origin of each electronic state of  $(\text{CO})_5$ , along with the excited vibrational progressions, is indicated.

**Table 1.** The Electron Binding Energies (EBEs in eV) of and the Vibrational Frequencies ( $\text{cm}^{-1}$ ) in the Observed Bands in the NIPE Spectra of  $(\text{CO})_5^{\bullet-}$  and  $(\text{CO})_6^{\bullet-}$ <sup>a</sup>

	peak (state) [sym]	EBE	EA/gap		vibrational frequency	
			exptl	calcd	exptl	calcd
$(\text{CO})_5$	X ( $^1A_1'$ ) [ $D_{5h}$ ]	3.830(5)	88.3 (EA)	87.4	1770, 540	1814, 508
	A ( $^3B_1$ ) [ $C_{2v}$ ]	4.68(1)	19.6 (X–A)	21.9 ( $\Delta E_{\text{ST}}$ )	1770, 1050	1821, 1028
$(\text{CO})_6$	X ( $^1A_1$ ) [ $D_{3d}$ ]	3.785(5)	87.3 (EA)	86.0	1730, 480	1802, 454
	A ( $^3B_1$ ) [ $D_2$ ]	4.70(1)	21.1 (X–A)	24.3 ( $\Delta E_{\text{ST}}$ )	1650	1801
	B	5.72(1)	23.5 (A–B)		1690	

<sup>a</sup>The experimental values of EA and  $\Delta E_{\text{ST}}$  (kcal/mol) are compared with those obtained from (RO)CCSD(T)/aug-cc-pVTZ//((U)B3LYP/6-311+G(2df) calculations, and the observed vibrational frequencies are compared with those obtained from B3LYP/6-311+G(2df) calculations.

is roughly half that of band A. Both bands show multiple, equally spaced, well-resolved fine structures, suggesting that each band is derived from a different electronic state of  $(\text{CO})_5$ , with the fine structure in each band being due to progressions from vibrational excitations. The larger intensity of band A indicates that it belongs to a triplet state, which has three spin components, whereas a singlet state has only one.<sup>8,19</sup> The assignment of band X to the lowest singlet state of  $(\text{CO})_5$  and band A to the triplet means that  $(\text{CO})_5$  has a singlet ground state.

Two vibrational progressions with frequencies of  $1770 \pm 40 \text{ cm}^{-1}$  (black lines) and  $1050 \pm 40 \text{ cm}^{-1}$  (shorter blue lines) are discernible in band A at 193 nm (Figure 2b). Although only one vibrational progression of  $1770 \pm 40 \text{ cm}^{-1}$  is clearly visible in band X in Figure 2b, there are discernible shoulders on the high binding energy side of each of the main peaks. In fact, in the 266 nm spectrum in Figure 2a, an additional vibrational mode, with a frequency of  $540 \pm 40 \text{ cm}^{-1}$ , is resolved in the ground-state transition (X).

Calculations (vide infra) find the vibrations with the high and low frequencies in band X correspond, respectively, to the totally symmetric C=O and C–C stretching modes of  $(\text{CO})_5$  in the singlet ground state. In band A, the high-frequency vibration is again assigned to the totally symmetric C=O stretching mode, but the low-frequency vibration is assigned to a C–C stretching mode in the triplet that is different from the C–C stretching mode in the singlet.

The positions of the origin of each electronic state was determined from the first resolved peak to be  $3.830 \pm 0.005 \text{ eV}$  (X) and  $4.680 \pm 0.010 \text{ eV}$  (A). Thus, as shown in Table 1, the NIPE spectra of  $(\text{CO})_5^{\bullet-}$  in Figure 2 give EA = 3.83 eV (88.3 kcal/mol) for the singlet ground state of  $(\text{CO})_5$  and  $\Delta E_{\text{ST}} = 0.85 \text{ eV}$  (19.6 kcal/mol) for the energy of the triplet excited state, relative to the singlet ground state. The high accuracy for the energy of the X feature is possible, because its position is located right between two peaks in the NIPE spectrum of  $\Gamma^-$ , so that the energy of X can be accurately calibrated.

Three electronic transitions, X, A, and B, are seen in the 193 nm spectrum of  $(\text{CO})_6^{\bullet-}$  (Figure 3b). Respectively, these bands have binding energies of  $3.785 \pm 0.005$ ,  $4.70 \pm 0.01$ , and  $5.72 \pm 0.01 \text{ eV}$  and show vibrational progressions with frequencies of  $1730 \pm 40$  (X),  $1650 \pm 40$  (A), and  $1690 \pm 40 \text{ cm}^{-1}$  (B). Calculations assign these frequencies to the excitation of symmetrical C=O stretching vibrations (vide infra).

The ground-state transition (X) is better resolved in the 266 nm NIPE spectrum (Figure 3a). This spectrum shows one additional vibrational excitation, with a frequency of  $480 \pm 40 \text{ cm}^{-1}$ , which is assigned to the totally symmetric C–C stretching mode in  $(\text{CO})_6$ .

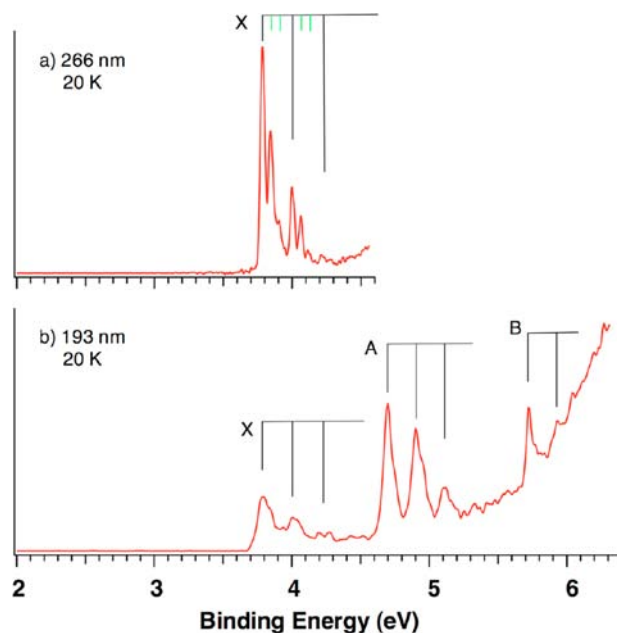


**Figure 3.** Low-temperature (20 K) NIPE spectra of  $(\text{CO})_6^{\bullet-}$  at (a) 266 and (b) 193 nm. The origin position of each electronic state of  $(\text{CO})_6$ , along with the excited vibrational progressions, is indicated.

The A transition exhibits the strongest intensity, while X and B show similar peak heights, again suggesting singlet electronic states for X and B and a triplet state for A.<sup>8,19</sup> Thus, as shown in Table 1, the NIPE spectra of  $(\text{CO})_6^{\bullet-}$  in Figure 3 give EA = 3.785 eV (87.3 kcal/mol) for the singlet ground state of  $(\text{CO})_6$  and  $\Delta E_{\text{ST}} = 0.915 \text{ eV}$  (21.1 kcal/mol) for the energy of the triplet excited state, relative to the singlet ground state.

**Optimized Structures and Calculated EA and  $\Delta E_{\text{ST}}$  Values.** In order to confirm our analyses of the NIPE spectra of  $(\text{CO})_5^{\bullet-}$  and  $(\text{CO})_6^{\bullet-}$ , we carried out high-quality, ab initio calculations. In addition, having very accurate experimental determinations of EA and  $\Delta E_{\text{ST}}$  for  $(\text{CO})_5$  and  $(\text{CO})_6$  from the NIPE spectra allowed us to test the ability of our calculations to reproduce the experimental values.

The (U)B3LYP/6-311+G(2df) optimized geometries of  $(\text{CO})_5^{\bullet-}$  and the lowest singlet state of  $(\text{CO})_5$  have  $D_{5h}$  symmetry. However, the lowest triplet and open-shell singlet states of the neutral are both degenerate ( $E_2''$ ),<sup>6</sup> so they each undergo a first-order Jahn–Teller distortion<sup>20</sup> to  $C_{2v}$  symmetry. The optimized C–C and C=O bond lengths in  $(\text{CO})_5^{\bullet-}$  and in each of these three electronic states of  $(\text{CO})_5$  are given in Figure 4.

(U)B3LYP/6-311+G(2df) geometry optimizations lead to a  $D_2$  structure for  $(\text{CO})_6^{\bullet-}$  and to  $D_{3d}$ ,  $D_2$ , and  $D_2$  structures for

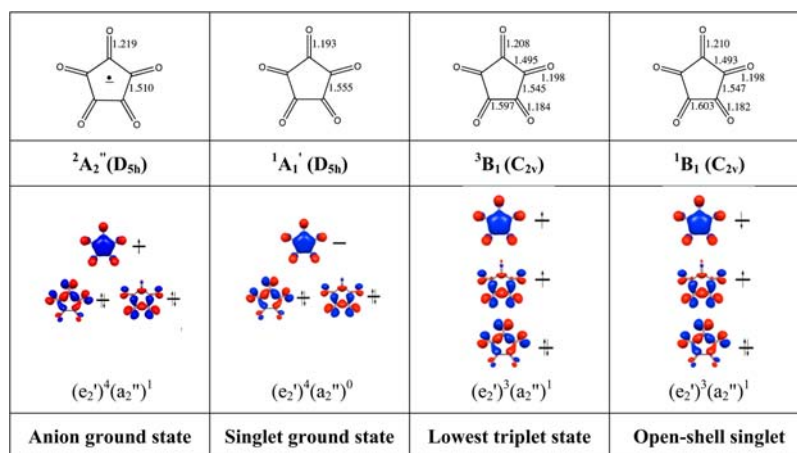


**Figure 4.** Geometries of the  $(\text{CO})_5^{\bullet-}$  radical anion and the singlet and triplet states of  $(\text{CO})_5$ , optimized at the (U)B3LYP/6-311+G(2df) level. The MOs are classified in  $D_{5h}$  symmetry.

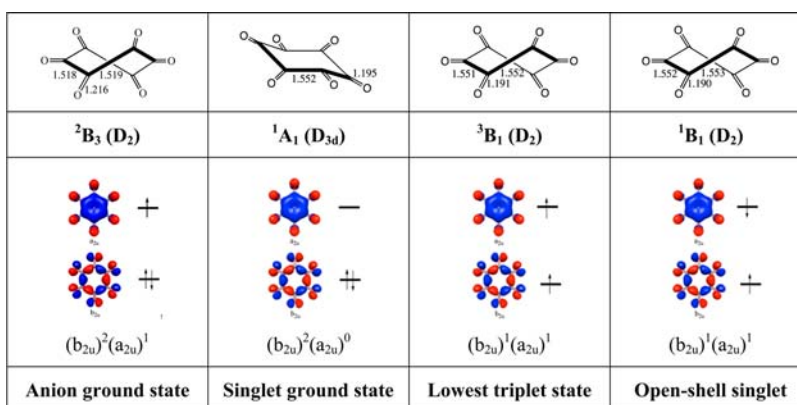


**Figure 5.** Geometries of the  $(\text{CO})_6^{\bullet-}$  radical anion and the singlet and triplet states of  $(\text{CO})_6$ , optimized at the (U)B3LYP/6-311+G(2df) level. The MOs are described in  $D_{6h}$  symmetry.

the ground-state singlet, triplet, and open-shell singlet states, respectively, of the neutral  $(\text{CO})_6$  molecule. The optimized geometries, including the C—C and the C=O bond lengths, are given in Figure 5.

Single-point EA and  $\Delta E_{\text{ST}}$  values for  $(\text{CO})_5$  and  $(\text{CO})_6$  were calculated at many different levels of theory. The energies obtained from those calculations are contained in Tables S1–S4 of the Supporting Information. We believe that the most reliable EA and  $\Delta E_{\text{ST}}$  values are those obtained from the differences between single-point energies that were computed at the (RO)CCSD(T)/aug-cc-pVTZ//(U)B3LYP/6-311+G(2df) level of theory. These calculated values are given in Table 1,<sup>21</sup> where they are compared with the experimental EA and  $\Delta E_{\text{ST}}$  values, obtained from the NIPE spectra.

The results in Table 1 show that our (RO)CCSD(T)/aug-cc-pVTZ//(U)B3LYP/6-311+G(2df) calculations give EA values that are approximately 1 kcal/mol lower and  $\Delta E_{\text{ST}}$  values that are 2–3 kcal/mol higher than those obtained from the NIPE spectra. The good agreement between the calculated and measured values of EA and  $\Delta E_{\text{ST}}$  provides support for our assignments of the X and A peaks in the  $(\text{CO})_5^{\bullet-}$  and  $(\text{CO})_6^{\bullet-}$  spectra as being due to the transitions from the ground state of each radical anion to the lowest singlet and triplet states, respectively, of the corresponding neutrals.

The next excited state in each neutral that might be accessed by NIPES is predicted to be the open-shell singlet state, in

which the two unpaired electrons occupy the same MOs as in the triplet state but with opposite spins (Figures 4 and 5). This open-shell singlet state is calculated to be approximately 6 kcal/mol for  $(\text{CO})_5$  and 4 kcal/mol for  $(\text{CO})_6$  higher in energy than the lowest triplet state.

It might be supposed that the peak in the NIPE spectrum of  $(\text{CO})_5^{\bullet-}$  at an EBE of 4.81 eV could be due to a transition to this open-shell singlet state. However, the calculated energy differences between the triplet and the open-shell singlet state of  $(\text{CO})_5$  are 6.2, 6.4, and 5.9 kcal/mol, using the CCSD(T), CASPT2, and RASPT2 methods, respectively (Table S5–S9, Supporting Information). These calculated energy differences are roughly twice as large as the energy difference of 0.13 eV (3.0 kcal/mol) between peak A and the peak at an EBE of 4.81 eV in the  $(\text{CO})_5^{\bullet-}$  spectrum. This difference of a factor of 2 makes assignment of the peak at EBE = 4.81 eV to the open-shell singlet state questionable.

If this assignment were correct, a similar peak, slightly higher in energy than peak A, would have been expected to have been seen in the NIPE spectrum of  $(\text{CO})_6^{\bullet-}$  in Figure 3b. The absence of such a peak, from the  $(\text{CO})_6^{\bullet-}$  NIPE spectrum in Figure 3b, also disfavors the open-shell singlet assignment of the peak at EBE = 4.81 eV in the  $(\text{CO})_5^{\bullet-}$  NIPE spectrum in Figure 2b. Indeed, we believe that the transitions to the open-shell singlet states are not seen in the NIPE spectra of either  $(\text{CO})_5^{\bullet-}$  or  $(\text{CO})_6^{\bullet-}$  and that these bands are most likely

buried under the more intense triplet peaks in the NIPE spectra in Figures 2b and 3b.

If the peak at EBE = 4.81 eV in the  $(\text{CO})_5^{\bullet-}$  NIPE spectrum is not due to the open-shell singlet, to what is this peak due? One possible assignment would be as the first peak in a vibrational progression of about  $1050\text{ cm}^{-1}$  in the triplet state of  $(\text{CO})_5$ . This assignment would also explain the peak at about  $1050\text{ cm}^{-1}$  above the first peak in the  $1770\text{ cm}^{-1}$  vibrational progression in the triplet state. The presence of this  $1050\text{ cm}^{-1}$  progression in the triplet band in the NIPE spectrum of  $(\text{CO})_5^{\bullet-}$  and the absence of this  $1050\text{ cm}^{-1}$  progression from the triplet band in the NIPE spectrum of  $(\text{CO})_6^{\bullet-}$  might then be attributable to the Jahn–Teller distortion<sup>20</sup> that is predicted to be present in the triplet state of  $(\text{CO})_5$  but absent from the triplet state of  $(\text{CO})_6$ .

**FCFs Simulations and Vibrational Analyses.** In order to better understand the vibrational fine structure in the NIPE spectra of  $(\text{CO})_5^{\bullet-}$  and  $(\text{CO})_6^{\bullet-}$ , particularly in the triplet bands in these spectra, and to confirm the assignments of the bands in the previously published NIPE spectrum of  $(\text{CO})_4^{\bullet-}$ ,<sup>5</sup> we calculated the FCFs for the NIPE spectra of  $(\text{CO})_n^{\bullet-}$ ,  $n = 4$ –6. Expanded versions of the experimental spectra and our computational simulations of the vibrational structures in them are given in Figures 6–8.

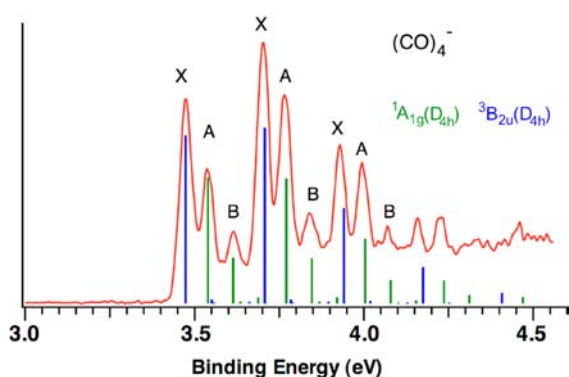


**Figure 6.** Simulated vibrational structure in the NIPE spectrum of  $(\text{CO})_4^{\bullet-}$ , superimposed onto the experimental spectrum. Note that only two electronic transitions, i.e., to the  ${}^3\text{B}_{2u}$  ground state (blue lines) and to the low-lying  ${}^1\text{A}_{1g}$  excited state (green lines), were used in the simulation. The simulation shows that the B peaks are not due to a third electronic state but are part of a vibrational progression in the symmetrical C–C stretching mode in the closed-shell  ${}^1\text{A}_{1g}$  state.

$(\text{CO})_4^{\bullet-}$ . The ground state of  $(\text{CO})_4^{\bullet-}$  and the triplet and two low-lying singlet states of  $(\text{CO})_4$  are all predicted to have  $D_{4h}$  structures.<sup>1,2</sup> The simulation of the vibrational structure in the NIPE spectrum of  $(\text{CO})_4^{\bullet-}$  was carried out for  ${}^2\text{A}_{2u} \rightarrow {}^3\text{B}_{2u}$  (blue lines) and  ${}^2\text{A}_{2u} \rightarrow {}^1\text{A}_{1g}$  (green lines). The 0–0 lines for each state were set to the experimental values (i.e., X = 3.475 eV, and A = 3.54 eV).<sup>5</sup> In Figure 6, the simulated stick spectrum is superimposed onto the 20 K, 266 nm NIPE spectrum.

In the simulation, the X and A bands are both calculated to show a vibrational progression of  $\sim 1800\text{ cm}^{-1}$  that corresponds to the symmetric C=O stretching mode. However, in addition to this mode, the simulated spectrum shows a relatively strong vibrational progression in the  ${}^1\text{A}_{1g}$  state, corresponding to the symmetric C–C stretching mode ( $603\text{ cm}^{-1}$ ). As shown in Figure 6, this progression aligns perfectly with the B series of peaks in the experimental spectrum.

On the basis of the apparent absence of a similar progression from peak X in the NIPE spectrum of  $(\text{CO})_4^{\bullet-}$ , a provisional assignment of the group of B peaks to the open-shell  ${}^1\text{B}_{2u}$  state was previously made.<sup>5</sup> However, Figure 6 shows that the group of B peaks actually corresponds to a vibrational progression in the symmetrical C–C stretching mode in the closed-shell  ${}^1\text{A}_{1g}$  state. Therefore, all the peaks in the experimental NIPE spectrum of  $(\text{CO})_4^{\bullet-}$  can be accounted for, without having to invoke a contribution to the spectrum from the  ${}^1\text{B}_{2u}$  state.

The reassignment of the B peaks to a vibrational progression in the symmetrical C–C stretching mode in the closed-shell  ${}^1\text{A}_{1g}$  state raises the following question: why is the same type of vibrational progression not also seen in band X for the ground  ${}^3\text{B}_{2u}$  state? Careful inspection of the baseline in the calculated stick spectrum in Figure 6 shows that the same vibrational progression does in fact exist in the  ${}^3\text{B}_{2u}$  state, but the lines for this progression are calculated to be about a factor of 10 less intense than the lines for the corresponding progression in the  ${}^1\text{A}_{1g}$  excited state.

The difference between the calculated intensities of the lines for this symmetrical C–C stretching progression in these two states of  $(\text{CO})_4$  can be attributed to a smaller difference between the calculated C–C bond lengths in the  ${}^2\text{A}_{2u}$  state of  $(\text{CO})_4^{\bullet-}$  ( $R = 1.515\text{ \AA}$ ) and in the  ${}^3\text{B}_{2u}$  state of  $(\text{CO})_4$  ( $R = 1.554\text{ \AA}$ ), compared to the difference between the calculated C–C bond lengths in the  ${}^2\text{A}_{2u}$  state of  $(\text{CO})_4^{\bullet-}$  and in the  ${}^1\text{A}_{1g}$  state ( $1.570\text{ \AA}$ ) of  $(\text{CO})_4$ . The larger the difference between the lengths of a particular bond in the radical anion and an electronic state of the neutral molecule, the larger are the FCFs for the bands in the progression for a vibration that affects this bond length.<sup>23</sup>

$(\text{CO})_5^{\bullet-}$ . The calculated positions and intensities of the peaks in the vibrational progressions in the X band ( $D_{5h}$ ,  $A_1'$ , singlet state) of  $(\text{CO})_5^{\bullet-}$  correspond quite well with those observed in the high-resolution (266 nm) NIPE spectrum (Figure 7). The higher frequency progression (black lines) is assigned to the symmetric C=O stretching mode, with a calculated frequency of  $1814\text{ cm}^{-1}$ . The lower frequency progression (light green lines) is assigned to the symmetric C–C stretching mode, with a calculated frequency of  $508\text{ cm}^{-1}$ .

The simulated positions for the A and B bands in the low-resolution (193 nm) spectrum of  $(\text{CO})_5^{\bullet-}$  also fit well the positions of these bands in the experimental spectrum. The higher frequency progression, A, is again assigned to the symmetric C=O stretching mode, with a calculated frequency of  $1821\text{ cm}^{-1}$ . The lower frequency progression, B, corresponds to a C–C stretching mode in the  $\text{C}_{2v}$  triplet state, with a calculated frequency of  $1028\text{ cm}^{-1}$ .

Why is there a factor of 2 difference between the frequencies of the progressions for C–C stretching in the singlet ground state and triplet excited state? The answer is that they are different types of C–C stretching vibrations. The C–C stretching progression in the singlet is for  $a_1'$  ring breathing, a vibrational mode that preserves the  $D_{5h}$  symmetry that is common to the optimized geometries of the  ${}^2\text{A}_2''$  ground state of  $(\text{CO})_5^{\bullet-}$  and the  ${}^1\text{A}_1'$  ground state of  $(\text{CO})_5$ .

In contrast, the C–C stretching progression in the triplet is for a vibrational mode that distorts the molecular geometry from the  $D_{5h}$  symmetry of the  ${}^2\text{A}_2''$  state of  $(\text{CO})_5^{\bullet-}$  to the  $\text{C}_{2v}$  symmetry of the Jahn–Teller distorted  ${}^3\text{E}_2''$  state of  $(\text{CO})_5$ .<sup>20,24</sup> It is along this symmetry breaking distortion coordinate that the equilibrium C–C bond lengths of the radical anion and

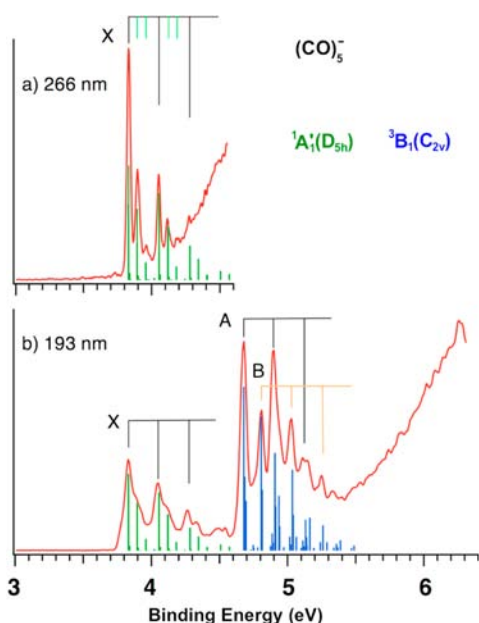


**Figure 7.** Simulated vibrational structure in the NIPE spectrum of  $(\text{CO})_5^{\bullet-}$ , superimposed onto the experimental spectrum. Note that only two electronic transitions, i.e., to the  ${}^1A_1'$  ground state (green lines) and to the lowest-lying  ${}^3B_1$  excited state (blue lines), were used in the simulation. The simulation shows that the B peaks are part of a vibrational progression in a C—C stretching mode in the  $C_{2v}$  triplet state.

triplet differ most. Consequently, this C—C vibrational mode is active in the band for formation of the triplet state of  $(\text{CO})_5$  in the NIPE spectrum of  $(\text{CO})_5^{\bullet-}$ .

$(\text{CO})_6^{\bullet-}$ . The simulation of the  $(\text{CO})_6^{\bullet-}$  NIPE spectrum proved more problematic than the simulations of the  $(\text{CO})_4^{\bullet-}$  and  $(\text{CO})_5^{\bullet-}$  NIPE spectra. Although the optimized geometries of the  $(\text{CO})_6^{\bullet-}$  radical anion and the triplet state of  $(\text{CO})_6$  both have  $D_2$  symmetry, the optimized geometry of the singlet state has  $D_{3d}$  symmetry. The presence of the 3-fold axis of symmetry in the  $D_{3d}$  geometry of the singlet prevented ezSpectrum from obtaining a diagonal vibrational overlap matrix, thus causing the generation of the vibrational spectrum for the singlet to fail.

In order to circumvent this problem, the simulation of the singlet portion of the  $(\text{CO})_6^{\bullet-}$  NIPE spectrum was performed, using the optimized  $D_2$  geometries for both the radical anion and the singlet. The B3LYP/6-311+G(2df) optimized  $D_2$  geometry of the singlet is only 0.3 kcal/mol higher in energy than the  $D_{3d}$  geometry.

The calculated positions of the lines in the X band (singlet state) correlate well with those in the high-resolution (266 nm) experimental spectrum. The simulation shows that the 0–0 band is not the most intense band in the spectrum. The intensity of the 0–0 line is calculated to be about a factor of 2 smaller than the most intense line, which arises from excitation of a low-frequency ( $44\text{ cm}^{-1}$ ) planarization mode. Therefore, the 0–0 line in the simulated spectrum is 0.005 eV lower in energy than the most intense line. The simulation shows that the major progressions in the high-resolution 266 nm spectrum are composed of a set of combination bands, involving three different vibrations: the low-frequency planarization mode ( $44\text{ cm}^{-1}$ ), the symmetric C=O bond stretch ( $1801\text{ cm}^{-1}$ ), and a symmetric C—C stretching mode ( $453\text{ cm}^{-1}$ ).

The calculated positions of the lines in the triplet state also correspond well to the positions of the A bands in the low-resolution (193 nm) spectrum. The simulation again shows that the 0–0 line is not the most intense line in the triplet. The intensity of the 0–0 line is calculated to be about a factor of 10 smaller than the most intense line, which arises from excitation of a low-frequency ( $56\text{ cm}^{-1}$ ) planarization mode. The simulation shows that the major progressions in the A band in the low-resolution 193 nm spectrum are composed of a set of combination bands, involving the low-frequency planarization mode ( $56\text{ cm}^{-1}$ ) and the symmetric C=O bond stretch ( $1801\text{ cm}^{-1}$ ). The shoulders on the high-energy side of the A band are due to a symmetric C—C stretching mode ( $461\text{ cm}^{-1}$ ).

Figure 8 shows that, as in the case of  $(\text{CO})_4^{\bullet-}$  and  $(\text{CO})_5^{\bullet-}$ , the simulation of the vibrational structure in the NIPE spectrum of  $(\text{CO})_6^{\bullet-}$  provides a good fit to the experimental spectrum.

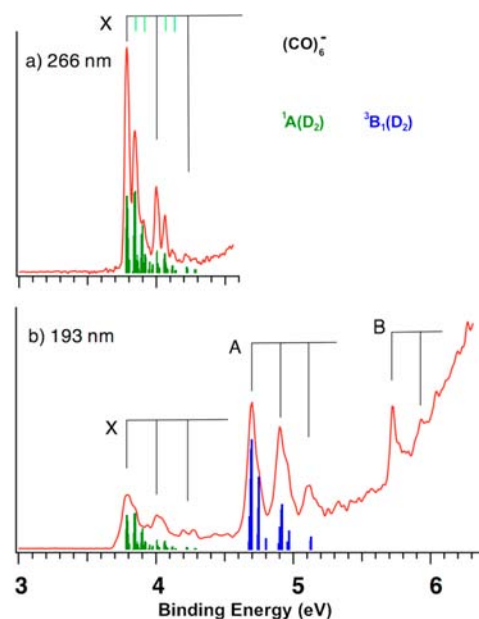


**Figure 8.** Simulated vibrational structure in the NIPE spectrum of  $(\text{CO})_6^{\bullet-}$ , superimposed onto the experimental spectrum. The simulated spectrum was obtained using the  $D_2$  optimized geometries for the singlet, as well as the radical anion and triplet states.

## CONCLUSIONS

In summary, we describe in this work the results of a study of the electronic states of  $(\text{CO})_5$  and  $(\text{CO})_6$  by a combination of NIPES and high-level electronic structure calculations. Not only do the calculations do a good job of reproducing the energies of the singlet and triplet bands in the NIPE spectra of  $(\text{CO})_5^{\bullet-}$  and  $(\text{CO})_6^{\bullet-}$ , but the calculations also provide very good simulations of the vibrational structure of each of the bands in the NIPE spectra of these two radical anions. The simulation of the vibrational structure in the previously published NIPE spectrum of  $(\text{CO})_4^{\bullet-}$  shows that all of the peaks in the experimental spectrum can be accounted for in terms of formation of only the triplet ground state, plus a closed-shell, singlet excited state.

The results of our calculations of both the position and the vibrational structure in each of the bands in the NIPE spectra of

(CO)<sub>5</sub><sup>•-</sup> and (CO)<sub>6</sub><sup>•-</sup>, strongly support our interpretations of the spectra. In turn, the spectra confirm the predictions, based on qualitative considerations of the electronic structures of (CO)<sub>5</sub> and (CO)<sub>6</sub>, that, unlike (CO)<sub>4</sub>,<sup>1b-e,2,5</sup> these two members of the (CO)<sub>n</sub> series of molecules should each have a singlet ground state.<sup>6</sup>

## ■ ASSOCIATED CONTENT

### ■ Supporting Information

Calculated EA and singlet–triplet energy differences for (CO)<sub>5</sub> and (CO)<sub>6</sub> at many different levels of theory (Tables S1–S4), optimized geometries (Figures S1 and S2) and relative energies (Tables S5 and S6) of four states of (CO)<sub>5</sub> and (CO)<sub>6</sub>, CASPT2 relative energies of the singlet, triplet, and open-shell singlet (Tables S7 and S8), RASPT2 and CCSD(T) calculations on (CO)<sub>5</sub> triplet and open-shell singlet energy gap (Table S9), and simulated stick photoelectron spectra of (CO)<sub>n</sub>, *n* = 4–6 (Tables S10–S12). This material is available free of charge via the Internet at <http://pubs.acs.org>.

## ■ AUTHOR INFORMATION

### Corresponding Author

borden@unt.edu; xuebin.wang@pnnl.gov

### Notes

The authors declare no competing financial interest.

## ■ ACKNOWLEDGMENTS

We thank Professor Laura Gagliardi for suggesting that we perform RASPT2 calculations on (CO)<sub>5</sub><sup>-</sup> and Professor Paul Wenthold for suggesting the use of ezSpectrum<sup>18</sup> for simulating the NIPE spectra. The calculations at UNT were supported by a grant CHE-0910527 from the National Science Foundation and by grant B0027 from the Robert A. Welch Foundation to W.T.B. The NIPES experiments at PNNL were supported by the Division of Chemical Sciences, Geosciences, and Biosciences, Office of Basic Energy Sciences, U.S. Department of Energy (DOE) and were performed using EMSL, a national scientific user facility sponsored by DOE's Office of Biological and Environmental Research and located at PNNL, which is operated by Battelle for DOE. X.B.W. would like to thank Professors Lai-Sheng Wang (Brown University, USA) and Si-Dian Li (Shanxi University, China) for discussions at the early stage of the experiments.

## ■ REFERENCES

- (1) (a) Gleiter, R.; Hyla-Kryspin, I.; Pfeifer, K.-H. *J. Org. Chem.* **1995**, *60*, 5878. (b) Jiao, H.; Frapper, G.; Halet, J.-F.; Saillard, J.-Y. *J. Phys. Chem. A* **2001**, *105*, 5945. (c) Zhou, X.; Hrovat, D. A.; Gleiter, R.; Borden, W. T. *Mol. Phys.* **2009**, *107*, 863. (d) Hansen, J. A.; Bauman, N. P.; Levine, B.; Borden, W. T.; Piecuch, P. Unpublished work. (e) Bartlett, R. J. Personal communication.
- (2) Zhou, X.; Hrovat, D. A.; Borden, W. T. *J. Phys. Chem. A* **2010**, *114*, 1304.
- (3) (a) Davidson, E. R.; Borden, W. T. *J. Am. Chem. Soc.* **1977**, *99*, 2053. (b) Review: Borden, W. T. *Diradicals*; Wiley: New York, 1982; pp 1–72.
- (4) Reviews: (a) Borden, W. T.; Iwamura, H.; Berson, J. A. *Acc. Chem. Res.* **1994**, *27*, 109. (b) Kutzelnigg, W. *Angew. Chem., Int. Ed. Engl.* **1996**, *35*, 572. (c) Hrovat, D. A.; Borden, W. T. *J. Mol. Struct.: THEOCHEM* **1997**, *398*, 211. (d) Hrovat, D. A.; Borden, W. T. *Modern Electronic Structure Theory and Applications in Organic Chemistry*; Davidson, E. R., Ed.; World Scientific Publishing Company: Singapore, 1997; pp 171–195.

(5) Guo, J.-C.; Hou, G.-L.; Li, S. D.; Wang, X.-B. *J. Phys. Chem. Lett.* **2012**, *3*, 304.

(6) Bao, X.; Zhou, X.; Lovitt, C. F.; Venkatraman, A.; Hrovat, D. A.; Gleiter, R.; Hoffmann, R.; Borden, W. T. *J. Am. Chem. Soc.* **2012**, *134*, 10259.

(7) (a) Hirst, D. M.; Hopton, J. D.; Linnett, J. W. *Tetrahedron, Suppl.* **1963**, *2*, 15. (b) Gimarc, B. M. *J. Am. Chem. Soc.* **1970**, *92*, 266. (c) Bodor, N.; Dewar, M. J. S.; Harget, A.; Haselbach, E. *J. Am. Chem. Soc.* **1970**, *92*, 3854. (d) Haddon, R. C. *Tetrahedron Lett.* **1972**, *13*, 3897. (e) Fleischhauer, J.; Beckers, M.; Scharf, H.-D. *Tetrahedron Lett.* **1973**, *14*, 4275. (f) Beebe, N. H. F.; Sabin, J. R. *Chem. Phys. Lett.* **1974**, *24*, 389. (g) Haddon, R. C.; Poppinger, D.; Radom, L. *J. Am. Chem. Soc.* **1975**, *97*, 1645. (h) Raine, G. P.; Schaefer, H. F., III; Haddon, R. C. *J. Am. Chem. Soc.* **1983**, *105*, 194. (i) Frenking, G. *Angew. Chem., Int. Ed. Engl.* **1990**, *29*, 1410. (j) Janoschek, R. *J. Mol. Struct.* **1991**, *232*, 147. (k) Korkin, A. A.; Balkova, A.; Bartlett, R. J.; Boyd, R. J.; Schleyer, P. v. R. *J. Phys. Chem.* **1996**, *100*, 5702. (l) Schröder, D.; Heinemann, C.; Schwarz, H.; Harvey, J. N.; Dua, S.; Blanksby, S. J.; Bowie, J. H. *Chem.—Eur. J.* **1998**, *4*, 2550. (m) Talbi, D.; Chandler, G. S. *J. Phys. Chem. A* **2000**, *104*, 5872. (n) Wang, H.-Y.; Lu, X.; Huang, R.-B.; Zheng, L.-S. *J. Mol. Struct.* **2002**, *593*, 187. (o) Trindle, C. *Int. J. Quantum Chem.* **2003**, *93*, 286. (p) Maclagan, R. G. A. R. *J. Mol. Struct.* **2005**, *713*, 107. (q) Golovin, A. V.; Ponomarev, D. A.; Takhistov, V. V. *J. Comput. Methods Mol. Des.* **2011**, *1*, 14.

(8) Review: Lineberger, W. C.; Borden, W. T. *Phys. Chem. Chem. Phys.* **2011**, *13*, 11792.

(9) Wang, X. B.; Wang, L. S. *Rev. Sci. Instrum.* **2008**, *79*, 073108.

(10) B3LYP is a combination of Becke's 3-parameter hybrid exchange functional (B3)<sup>11</sup> with the electron correlation functional of Lee, Yang, and Parr (LYP).<sup>12</sup>

(11) Becke, A. D. *J. Chem. Phys.* **1993**, *98*, 5648.

(12) Lee, C.; Yang, W.; Parr, R. G. *Phys. Rev. B* **1988**, *37*, 785.

(13) Krishnan, R.; Binkely, J. S.; Seeger, R.; Pople, J. A. *J. Chem. Phys.* **1980**, *72*, 650.

(14) Frisch, M. J.; Trucks, G. W.; Schlegel, H. B.; Scuseria, G. E.; Robb, M. A.; Cheeseman, J. R.; Scalmani, G.; Barone, V.; Mennucci, B.; Petersson, G. A.; Nakatsuji, H.; Caricato, M.; Li, X.; Hratchian, H. P.; Izmaylov, A. F.; Bloino, J.; Zheng, G.; Sonnenberg, J. L.; Hada, M.; Ehara, M.; Toyota, K.; Fukuda, R.; Hasegawa, J.; Ishida, M.; Nakajima, T.; Honda, Y.; Kitao, O.; Nakai, H.; Vreven, T.; Montgomery, J. A., Jr.; Peralta, J. E.; Ogliaro, F.; Bearpark, M.; Heyd, J. J.; Brothers, E.; Kudin, K. N.; Staroverov, V. N.; Kobayashi, R.; Normand, J.; Raghavachari, K.; Rendell, A.; Burant, J. C.; Iyengar, S. S.; Tomasi, J.; Cossi, M.; Rega, N.; Millam, N. J.; Klene, M.; Knox, J. E.; Cross, J. B.; Bakken, V.; Adamo, C.; Jaramillo, J.; Gomperts, R.; Stratmann, R. E.; Yazyev, O.; Austin, A. J.; Cammi, R.; Pomelli, C.; Ochterski, J. W.; Martin, R. L.; Morokuma, K.; Zakrzewski, V. G.; Voth, G. A.; Salvador, P.; Dannenberg, J. J.; Dapprich, S.; Daniels, A. D.; Farkas, O.; Foresman, J. B.; Ortiz, J. V.; Cioslowski, J.; Fox, D. J. *Gaussian 09*, revision A.02; Gaussian, Inc.: Wallingford, CT, 2009.

(15) (a) Purvis, G. D.; Bartlett, R. J. *J. Chem. Phys.* **1982**, *76*, 1910.

(b) Raghavachari, K.; Trucks, G. W.; Pople, J. A.; Head-Gordon, M. H. *Chem. Phys. Lett.* **1989**, *157*, 479.

(16) (a) Dunning, T. H. *J. Chem. Phys.* **1989**, *90*, 1007. (b) Kendall, R. A.; Dunning, T. H.; Harrison, R. J. *J. Chem. Phys.* **1992**, *96*, 6796.

(17) Werner, H.-J.; Knowles, P. J.; Manby, F. R.; Schütz, M.; Celani, P.; Knizia, G.; Korona, T.; Lindh, R.; Mitrushenkov, A.; Rauhut, G.; Adler, T. B.; Amos, R. D.; Bernhardsson, A.; Berning, A.; Cooper, D. L.; Deegan, M. J. O.; Dobbyn, A. J.; Eckert, F.; Goll, E.; Hampel, C.; Hesselmann, A.; Hetzer, G.; Hrenar, T.; Jansen, G.; Köppl, C.; Liu, Y.; Lloyd, A. W.; Mata, R. A.; May, A. J.; McNicholas, S. J.; Meyer, W.; Mura, M. E.; Nicklass, A.; Palmieri, P.; Pflüger, K.; Pitzer, R.; Reiher, M.; Shiozaki, T.; Stoll, H.; Stone, A. J.; Tarroni, R.; Thorsteinsson, T.; Wang, M.; Wolf, A. *MOLPRO*, version 2010.1, 2010; see <http://www.molpro.net>.

(18) Mozhayskiy, V. A.; Krylov, A. I. *ezSpectrum*, version 3.0; see <http://iopshell.usc.edu/downloads>.

(19) (a) Clifford, E. P.; Wenthold, P. G.; Lineberger, W. C.; Ellison, G. B.; Wang, C. X.; Grabowski, J. J.; Vila, F.; Jordan, K. D. *J. Chem.*

*Soc., Perkin Trans. 2* **1998**, 1015. (b) Wang, X. B.; Woo, H. K.; Wang, L. S. *J. Chem. Phys.* **2005**, *123*, 051106.

(20) Jahn, H. A.; Teller, E. *Proc. R. Soc. London, Ser. A* **1937**, *161*, 220.

(21) Artfactual symmetry breaking results<sup>22</sup> in our ROCCSD(T) calculations finding energies for the  ${}^3B_1$  and  ${}^3A_2$  components of  ${}^3E_2''$  that are not exactly the same at  $D_{5h}$  geometries. The lower energy component is calculated to be  ${}^3B_1$ , and the value of  $\Delta E_{ST}$  in Table 1 is based on its energy.

(22) Review: Davidson, E. R.; Borden, W. T. *J. Phys. Chem.* **1983**, *87*, 4783.

(23) The calculated FCFs and the associated intensities for all of the totally symmetric vibrations in the triplet and in the lowest energy closed-shell singlet state of  $(CO)_n$ ,  $n = 4-6$ , are provided in the Supporting Information (Tables S10–S12).

(24) In  $D_{5h}$  symmetry, the Jahn–Teller active, distortion mode of the  ${}^3E_2''$  state of  $(CO)_5$  is an  $e_1'$  vibration.<sup>20</sup> However,  $e_1'$  and  $e_2'$  vibrations in  $D_{5h}$  symmetry both become  $a_1$  vibrations in  $C_{2v}$  symmetry and hence are mixed at the equilibrium geometry of the Jahn–Teller distorted triplet state. Therefore, the C–C vibration that is active in the triplet band of the NIPE spectrum of  $(CO)_5^{\bullet-}$  is a mixture of  $e_1'$  and  $e_2'$  vibrations in  $D_{5h}$  symmetry.